Agricultural and Forest Meteorology 247 (2017) 181–193

Contents lists available at ScienceDirect

Agricultural and Forest Meteorology

journal homepage: www.elsevier.com/locate/agrformet

Validating canopy clumping retrieval methods using hemispherical photography in a simulated *Eucalypt* forest

William Woodgate[a,b,c,*], John D. Armston[d,e,f], Mathias Disney[g,h], Lola Suarez[a,b], Simon D. Jones[a,b], Michael J. Hill[i,j], Phil Wilkes[a,b,k], Mariela Soto-Berelov[a,b]

[a] School of Mathematical and Geospatial Sciences, RMIT University, GPO Box 2476V, Melbourne, VIC 3001, Australia
[b] Cooperative Research Centre for Spatial Information, Carlton, VIC 3053, Australia
[c] Land and Water, Commonwealth Scientific and Industrial Research Organisation, Yarralumla, ACT, Australia
[d] Remote Sensing Centre, Science Delivery, Queensland Department of Science, Information Technology, and Innovation, 41 Boggo Road, QLD 4102, Australia
[e] Joint Remote Sensing Research Program, School of Geography, Planning and Environmental Management, University of Queensland, St. Lucia, QLD 4072, Australia
[f] Department of Geographical Sciences, University of Maryland, College Park, MD 20742, USA
[g] Department of Geography, University College London,Gower Street, London WC1E 6BT, UK
[h] NERC National Centre for Earth Observation, UK
[i] Department of Earth System Science and Policy, University of North Dakota, Clifford Hall, 9011, 4149 University Drive, Grand Forks, ND 58202, USA
[j] School of the Environment, Flinders University, Sturt Road, Bedford Park, South Australia 5042, Australia
[k] ITC, University of Twente, P.O. Box 217, NL-7000 AE Enschede, The Netherlands

ARTICLE INFO

Keywords:
Leaf Area Index
Clumping
Woody-to-total area
3D modelling
Hemispherical photography
Eucalypt

ABSTRACT

The so-called clumping factor (Ω) quantifies deviation from a random 3D distribution of material in a vegetation canopy and therefore characterises the spatial distribution of gaps within a canopy. Ω is essential to convert *effective* Plant or Leaf Area Index into *actual* LAI or PAI, which has previously been shown to have a significant impact on biophysical parameter retrieval using optical remote sensing techniques in forests, woodlands, and savannas. Here, a simulation framework was applied to assess the performance of existing *in situ* clumping retrieval methods in a 3D virtual forest canopy, which has a high degree of architectural realism. The virtual canopy was reconstructed using empirical data from a Box Ironbark Eucalypt forest in Eastern Australia. Hemispherical photography (HP) was assessed due to its ubiquity for indirect LAI and structure retrieval. Angular clumping retrieval method performance was evaluated using a range of structural configurations based on varying stem distribution and LAI. The CLX clumping retrieval method (Leblanc et al., 2005) with a segment size of 15° was the best performing clumping method, matching the reference values to within 0.05 Ω on average near zenith. Clumping error increased linearly with zenith angle to > 0.3 Ω (equivalent to a 30% PAI error) at 75° for all structural configurations. At larger zenith angles, PAI errors were found to be around 25–30% on average when derived from the 55–60° zenith angle. Therefore, careful consideration of zenith angle range utilised from HP is recommended. We suggest that plot or site clumping factors should be accompanied by the zenith angle used to derive them from gap size and gap size distribution methods. Furthermore, larger errors and biases were found for HPs captured within 1 m of unrepresentative large tree stems, so these situations should be avoided in practice if possible.

1. Introduction

The fluxes of radiation, heat and water in a vegetation canopy are primarily determined by the total amount of vegetation and spatial distribution, characterised by Plant and Leaf Area Index or 'PAI' and 'LAI' respectively (Law et al., 2001; Spanner et al., 1990). LAI is recognised as an essential climate variable and key input into global climate models among other applications (GCOS, 2011). It is usually defined as one half the total green leaf area per unit horizontal ground surface area (GCOS, 2011).

LAI is typically estimated indirectly *in situ* from optical remote sensing instruments, which measure the proportion and spatial distribution of gaps in plant canopies (see reviews by (Bréda, 2003; Jonckheere et al., 2004; Zheng and Moskal, 2009)). These methods often utilise a theoretical model of canopy gap probability, *Pgap*, to estimate LAI (Monsi and Saeki, 1965; Nilson, 1971; Woodgate et al.,

* Corresponding author at: Room 27, Level 11, Building 12, Remote Sensing Centre, School for Mathematical and Geospatial Sciences, RMIT University, Melbourne, Australia.
E-mail address: william.woodgate@rmit.edu.au (W. Woodgate).

http://dx.doi.org/10.1016/j.agrformet.2017.07.027
Received 26 February 2017; Received in revised form 3 July 2017; Accepted 31 July 2017
Available online 06 October 2017

2015a). The spatial distribution is characterised by the angular distribution of material in the canopy and the so-called clumping index or factor 'Ω', which describes the typically non-random (clumped) distribution of material in a canopy over a defined 3D volume (Chen and Black, 1991, 1992; Nilson, 1971).

Clumping factors can vary with spatial scale and viewing angle, and are typically in the range of 0.4–1 at the stand scale for broadleaf forests (Chen et al., 2005; Leblanc et al., 2005; Zhao et al., 2012). Clumping factors < 1 imply that canopy elements are arranged in such a way that more gaps are found than if they were distributed randomly. Conversely, clumping factors > 1 are associated with regularly distributed canopy elements, meaning a lower gap proportion than if they were distributed randomly. A clumping factor of 1 is associated with a theoretically random spatial distribution of canopy elements. A main assumption of the *Pgap* model is that the clumping factor is equal to 1 unless explicitly accounted for, and therefore the model provides an estimate of effective (non-clumped) PAI or LAI (Chen and Cihlar, 1995a). However, in forests a clumping factor of 1 is typically invalid due to the clumping of canopy elements at all scales, from shoot/twig, to branch, to crown, to whole canopy or stand (Chen and Black, 1991; Fournier et al., 1997; Pisek et al., 2011). This can lead to up to a 50% LAI underestimation if the clumping factor is 0.5 for example (Leblanc et al., 2005).

In situ clumping estimates are used to support calibration and validation activities of Earth Observation global LAI and clumping products (Fernandes et al., 2014; Pisek et al., 2015). *In situ* clumping retrieval methods are an area of ongoing development and research (see Section 2). The traditional approach to benchmark and evaluate retrieval method performance has been to compare with other *in situ* methods deemed to be most accurate, such as destructive harvesting, allometric relationships and litter traps (c.f. Leblanc et al., 2014). However, this approach is no longer viable when trying to achieve a high level of accuracy in the order of < 10% LAI uncertainty, especially given errors also arise in the benchmark *in situ* methods in forests and woody ecosystems where clumping is particularly important. For example, Chen et al. (1997) reported difficulty in keeping total LAI error budgets below 25% using the direct and semi-direct techniques of harvesting and extrapolation to larger areas via allometry. Similar error budgets have been reported for litter-trap collection methods (Kalácska et al., 2005). This high uncertainty tolerance is unacceptable for current LAI product calibration and validation accuracy targets, which aim to match within 20% of independently derived *in situ* estimates, with the requirement to improve that to within 5% for future applications (Fernandes et al., 2014).

Three-dimensional modelling and computer simulation frameworks are an attractive alternative to traditional field-based benchmarking approaches, e.g. Leblanc and Fournier (2014); Walter et al. (2003); Widlowski et al. (2015); Woodgate et al. (2016). These frameworks enable retrieval method accuracy to be quantified precisely using the known model 'truth' as a benchmark for comparison. Of the few framework studies that assess LAI and clumping retrieval methods, ray tracing models coupled with a limited degree of canopy architectural realism were typically employed. For example, Jonckheere et al. (2006) simulated Hemispherical Photography (HP) in beech and Scots pine forest canopies to evaluate the divergence of theoretical foliage distribution models to the reference model value. Walter et al. (2003) evaluated two angular clumping retrieval techniques using simulated HPs. Virtual scenes comprised flat foliage (10 cm × 10 cm × 1 cm dimensions) of varying densities and clustering percentage. Gonsamo and Pellikka (2009) utilised the virtual scenes from Walter et al. (2003) to investigate five clumping retrieval methods from HPs on level and sloped terrain. More recently, Leblanc and Fournier (2014) evaluated the accuracy of four indirect clumping retrieval methods. HPs were simulated in virtual forest scenes comprising a broad range of stand structures.

A main challenge of modelling frameworks is the adequate representation of canopy architectural realism, where the spatial distribution of gaps at all scales should closely reflect empirical data. These simulation studies cited above found retrieval methods need to be further tested under conditions where canopies better represent the structural properties of an actual forest stand, such as including internal branching structure. The advantage in this case is to permit better definition of the accuracy, strengths and limitations of these indirect estimation methods. Consequently, there is a need for more complex 3D models created specifically for this purpose that accurately reflect the tree and stand structure of real forests.

The primary objective of this study was to determine the accuracy of several clumping retrieval methods when applied to a mature Eucalypt woodland. HP was assessed due to its ubiquitous and low-cost use for indirect LAI and structural retrieval (Leblanc and Fournier, 2014). Secondary objectives included quantitatively determining how the accuracy of the clumping retrieval methods vary with view zenith angle, stem distribution, and stand LAI. A simulation framework was applied to a virtual forest canopy with a high degree of architectural realism reconstructed from empirical data, representative of a Box Ironbark Eucalypt forest in Eastern Australia (Woodgate et al., 2016).

This manuscript first reviews briefly the theoretical background of *in situ* clumping retrieval methods (Section 2). Next, the 3D modelling and simulation framework is presented (Section 3) enabling the evaluation of clumping method performance from HP's to a range of stem distributions and LAI values (Section 4). The paper concludes with a discussion on the practical implications and recommendations for users of *in situ* clumping retrieval methods (Sections 5 and 6).

2. Theoretical background: *in situ* clumping retrieval methods

Canopy clumping retrieval methods are used to determine the degree of non-randomness of an observed canopy. The following sections present a categorisation and description of *in situ* clumping retrieval methods, typically applied from measurements of gap size and gap size distribution. As such, the clumping factor is a function of view zenith angle and can be retrieved over narrow angle ranges from instrument measurements such as HP images (Leblanc and Chen, 2001; Leblanc and Fournier, 2014; Pisek et al., 2011).

2.1. Logarithmic averaging (Ω_{LX})

Lang and Xiang (1986) proposed a method to retrieve clumping based on logarithmic averaging, using finite segments '*k*' of gap size distribution measurements, hereafter referred to as LX or Ω_{LX}:

$$\Omega_{LX}(\theta) = \ln[\overline{Pgap(\theta)}]/\overline{\ln[Pgap(\theta)]} = n\ln[\overline{Pgap(\theta)}]/\sum_{k=1}^{n}\ln[Pgap_k(\theta)] \quad (1)$$

Where $\ln[\overline{Pgap(\theta)}]$ is the logarithm of averaged gap fraction over a predefined area (i.e. a proportion of a single measurement of gap sizes or multiple measurements), $\overline{\ln[Pgap(\theta)]}$ is the average logarithm of gap fraction over the same area. $Pgap_k(\theta)$ is the gap fraction of segment *k* relating to a sub-domain of the gap size measurement. For example, $k = 90^\circ$ equates to the 360° azimuth ring of a HP image being divided into four 90° segments containing gap and canopy pixels. The size of *k* should preferably be at least 10 times the mean canopy element width, typically corresponding to leaf size. Two assumptions are made: (i) the canopy elements at the *k* scale are distributed randomly, and (ii) segments contain gaps, due to the undefined logarithm of $Pgap_k = 0$.

Due to the undefined calculation of a logarithm with a null-gap segment, a gap value of half a pixel is assigned. The maximum LAI value within a segment therefore becomes a function of *k* and zenith angle. Gonsamo et al. (2010) proposed a clumping retrieval method based on the LX principle, that utilises the minimum segment size for which a gap is present, as opposed to a fixed segment size that could lead to null

gap segments. The implications of null gap segments and segment size are discussed later in Sections 5.1 and 5.2.

LX with a segment size 'k' ≈ 270 − 360° (azimuth view cap specific) is the clumping method typically applied to the LAI-2000/2200 instrument *Pgap* estimates (LI-COR, 2011). However, multiple measurements at the same location while rotating the view cap can be used to restrict 'k' to mimic HP azimuthal segment capabilities from a single measurement (Chianucci et al., 2014).

2.2. Gap size distribution (Ω_{CC})

The corrected 'CC' or 'Ω_{CC}' Chen and Cihlar (1995b) method modified by Leblanc (2002) enables clumping retrieval through gap size distribution information, given as:

$$\Omega_{CC}(\theta) = \left[\frac{\ln[Pgap(\theta)]}{\ln[F_{mr}(\theta, 0)]}\right] \cdot \left[\frac{1 - F_{mr}(\theta, 0)}{1 - Pgap(\theta)}\right] \quad (2)$$

Where $Pgap(\theta)$ is the overall gap probability, $F_{mr}(\theta, 0)$ is the gap probability after removing large 'non-random' gaps. $F_{mr}(\theta)$ is obtained by the sequential removal of large non-random gaps that are not statistically possible for a given *Pgap*, until the pattern of gap size distribution resembles that of an equivalent canopy with a random spatial distribution of canopy elements. This is a key assumption of the method. CC is the clumping method typically employed by the TRAC instrument (Leblanc, 2002; Leblanc et al., 2005).

Variations of the CC method include: an approximation of the CC method by Walter et al. (2003), termed 'CCW'; and a modified CC method termed 'CMN' by Pisek et al. (2011), based on the original equation by Miller and Norman (1971), which does not consider a normalization factor for the non-gap proportion after the removal of large gaps (Leblanc, 2002). However, Leblanc and Fournier (2014) demonstrated the CMN method produced similar results to the CC method, but found it to be less reliable at low PAI values (< ≈2–3 PAI) in the virtual scenes tested.

2.3. Combined logarithmic averaging and gap size distribution (Ω_{CLX})

Leblanc et al. (2005) combined the logarithmic averaging and gap size distribution methods, termed 'CLX or Ω_{CLX}', to address the potentially limiting assumption of a random distribution of canopy elements at the segment scale associated with the LX method. The overall clumping index is then calculated over *n* segments:

$$\Omega_{CLX}(\theta) = \frac{n \ln[\overline{Pgap(\theta)}]}{\sum_{k=1}^{n} \ln[Pgap_k(\theta)]/\Omega cc_k(\theta)} \quad (3)$$

Where $\Omega_{CCk}(\theta)$ is the CC method (Eq. (2)) applied to the segment scale '*k*'.

2.4. Other clumping retrieval methods

Although the previously outlined clumping methods are more prevalent in the literature (Gonsamo and Pellikka, 2009; Gonsamo et al., 2011; Pisek et al., 2011), others have been proposed which aim to characterise the spatial distribution of canopy elements. However, some of these methods result in clumping factors that are not strictly applicable to LAI estimation from the *Pgap* formulation. For example, Frazer et al. (2005) developed a technique to determine fine-scale forest heterogeneity, based on lacunarity analysis. However, the authors concluded further research is required to understand how statistical estimates and gradients of measured heterogeneity relate to other ecological metrics such as forest structure. The Pielou coefficient of segregation (Pielou, 1962) has been applied to HP imagery to explore spatial dispersion of canopy elements based on *Pgap* and gap size distribution (Gonsamo et al., 2011; Pisek et al., 2011; Walter et al., 2003). Jonckheere et al. (2006) utilised a fractal-dimension based modelling approach to improve clumping factors of theoretical foliage distribution models. Clumping factors have also been retrieved from empirical equations (Kucharik et al., 1999) and theoretical models (Nilson, 1999).

Methods that incorporate ranging information from instruments such as terrestrial laser (LiDAR) scanners (TLS) have also been more recently developed to aid in clumping retrieval or to minimise the impact of clumping on indirect PAI estimation. Jupp et al. (2009) developed a PAI inversion method from TLS ranging data that subsumes some clumping effects via logarithmic averaging. They suggested multiple areas for improvement including separating between-crown gaps from within-crown gaps. Zhao et al. (2012) developed a nominal spatial extent index (NSEI) to characterise within-crown and between-crown gaps and then applied the results to the CC method (Eq. (2)). This manuscript does not focus on the field measurement method to determine gap probability, rather the processing techniques to derive clumping based on the gap size and distribution.

3. Materials and methods

3.1. 3D modelling of virtual scenes

The Rushworth 3D virtual forest reconstructed in Woodgate et al. (2015b) was selected for analysis. Rushworth forest located in Victoria (Australia, 36°45′S, 144°58′E) is representative of a dry sclerophyll forest comprised of several Eucalypt tree species. The trees are typically 10–15 m tall with an average stem density of 520 stems ha^{-1}. The single strata site is also characterised by low-lying undulating terrain and a lack of understorey. The 3D trees were reconstructed from empirical data to reproduce key structural attributes of Eucalypt species such as their moderate degree of within-crown clumping and predominant erectophile leaf angle distribution (Jacobs, 1955). More information on the Rushworth forest study site and tree reconstruction method can be found in Woodgate et al. (2015b).

A total of 24 virtual scenes were generated, comprising a combination of six different stem distributions and four scene PAI values (Fig. 1). Specifically, one regular, one random, and four clumped stem distributions with varying degrees of clumping were implemented for each scene PAI value (PAI = 0.6, 1.2, 1.8, and 2.4). The Neyman Type A distribution was used to parameterise the stem distributions of the clumped scenes, which is based on a double-Poisson distribution (Neyman, 1939), and has been used to adequately model clumped stem distributions of forests (Franklin et al., 1985). For every stem distribution a variance:mean '*v:m*' ratio is provided, which characterises the degree of stem clumping. Similar to the clumping factor, a *v:m* equal to 1 is theoretically equivalent to the Poisson or random distribution, *v:m* > 1 is associated with a clumped distribution, and *v:m* < 1 is associated with a regular or plantation style stem distribution.

Scenes were populated from a database of 51 unique spatially explicit tree models reconstructed from empirical data (Woodgate et al., 2015a). Trees were cloned to produce the desired scene stem density (see Table 1 in (Woodgate et al., 2016)). The exact same tree models were used for scenes with the same PAI. Additionally, scenes with PAI = 1.2 and 1.8 used the same tree models as the PAI = 0.6 scenes but with double and triple the frequency, respectively (Fig. 1). This critical step resulted in keeping within-crown clumping constant across virtual scenes, thus eliminating the potential for bias. The exception to this was PAI = 2.4 scenes, where a different proportional composition of tree models was implemented, using the same stem density as PAI = 1.8 scenes and substituting trees with low total leaf area with trees with high total leaf area. Here, priority was given to simulations of realistic stem density scenarios guided by field measurements over unrealistic scenarios. The average within-crown clumping factor for PAI = 2.4 scenes was within 0.01 of all other scenes for the 0° and 57.5° angles (see Woodgate et al. (2015a) for within-crown Ω), thus the overall effect on scene clumping from changing the composition of tree models comprising the PAI = 2.4 scenes is likely negligible.

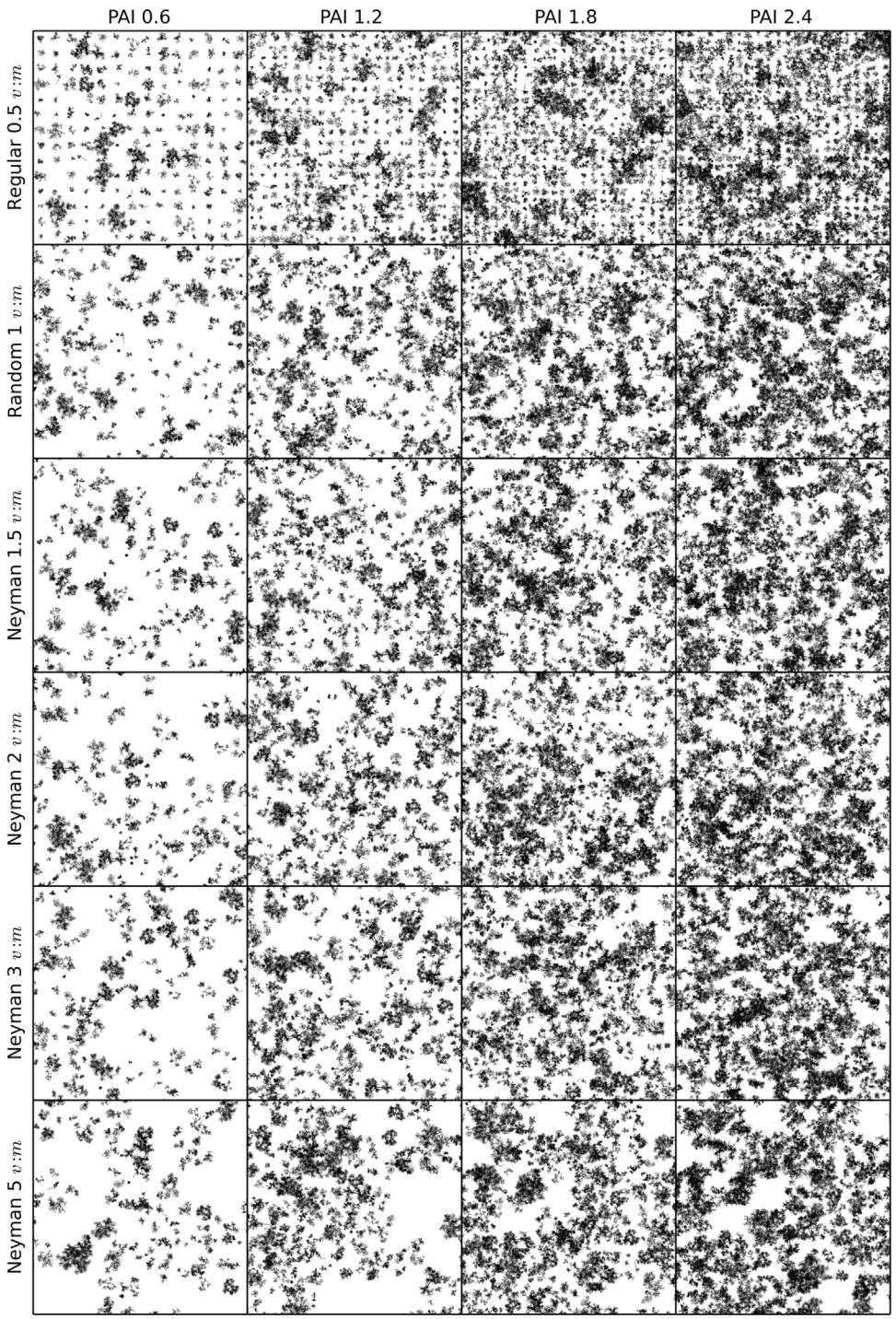

Fig. 1. Scene element cover maps depicting the stem distributions. 90 m × 90 m binary element cover maps of all 24 simulated scenes; comprising four PAI values (columns) and six stem distributions (rows), ordered by variance to mean (*v:m*) stem clumping value. The simulated cover map resolution was 1 cm × 1 cm.

Edge effects (i.e. loss of simulated fluxes from finite scene boundaries) were avoided by cloning the original 90 m × 90 m scene domain to produce a 270 m × 270 m scene domain in a 3 × 3 grid configuration. More information on the virtual scene composition and validation with empirical measurements can be found in (Woodgate et al., 2016).

3.2. Simulation of hemispherical photographs (HPs) and canopy cover maps

In each virtual scene, 13 HPs were simulated using the librat ray-tracing model (Disney et al., 2011; Lewis, 1999). The sampling scheme implemented was derived from the State-wide Landcover and Trees Study (SLATS) transects, developed to estimate foliage projective cover (among other metrics) for calibration and validation of remotely sensed products (Armston et al., 2009; Schaefer et al., 2015). HPs were simulated 25 m apart on three intersecting 100 m transects, oriented at 60 ° from one another (see Fig. 1 from Woodgate et al. (2016)). The centre of the sampling design was coincident with the centre of the 270 m × 270 m scene domain. HPs were simulated at 1.5 m above ground level, pointing directly upwards with 180° hemispherical field-of-view (FOV) with a cosine lens projection (Fig. 2). A minimum separation distance of 30 cm between HP measurement and tree stem location was ensured. The HP image resolution was set to 3001 × 3001 pixels, which is equivalent to a 12 megapixel digital camera with a 4:3 image format.

HPs were simulated in ‘reference’ mode in librat to simulate true

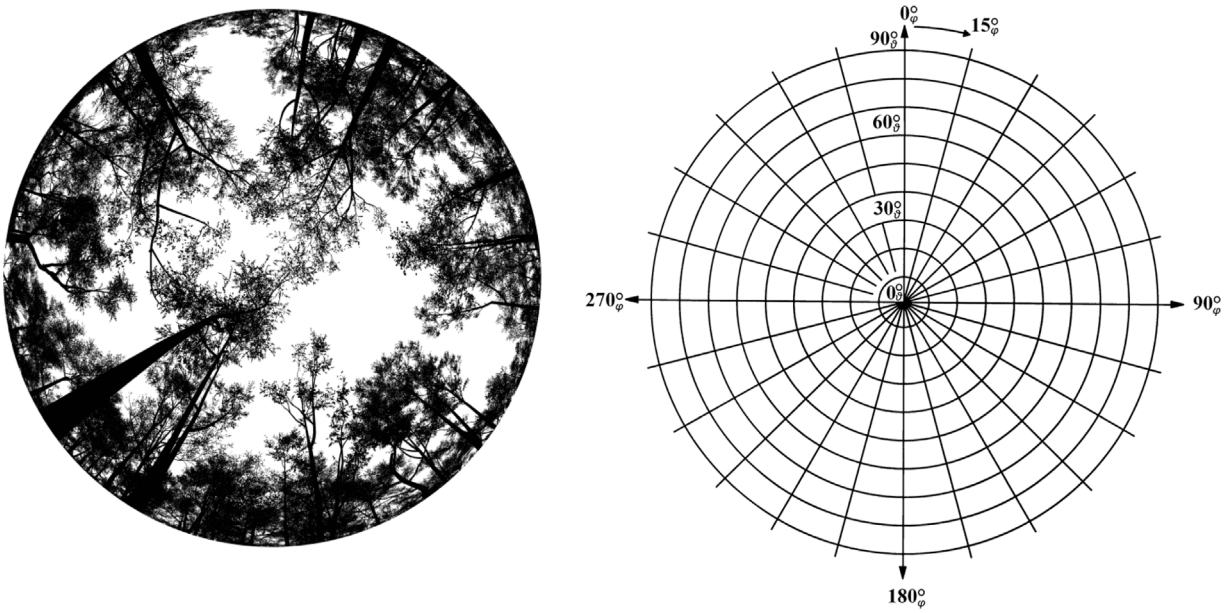

Fig. 2. A simulated HP image in reference mode (left); polar plot demonstrating zenith angle 'θ' and azimuth angle 'φ', using 10° zenith bins and 15° azimuth bins relating to 'k' segment size = 15° (right).

gap fraction determined from ray intersection. For every pixel in the image FOV, a single ray is traced from the camera position in the direction of the pixel centroid to determine if there is a canopy intersection event returning a binary result; '0' for a canopy intercept or '1' for a gap. This method effectively produces pre-classified 'reference' HP images, thus avoiding potential *Pgap* classification errors that would otherwise confound interpretation of results. More information on the simulation of HPs can be found in Woodgate et al. (2016).

Virtual scene cover maps (90 m × 90 m) were simulated in *librat* at 1 cm resolution, based on a solitary ray traced at the centroid of each pixel returning the first intercept height from above the canopy. Similar to the simulated HPs, these cover maps can be treated as reference *Pgap* free from numerous potential sources of error (Armston, 2013).

3.3. Clumping retrieval method performance evaluation

The LX, CC, CCW and CLX clumping retrieval methods (described above in Section 2) were evaluated. Only clumping retrieval methods applicable to 2D gap size measurements from instruments such as the TRAC, and LAI-2000/2200, or HP methods were investigated. The clumping retrieval method values were computed using DHP.exe version 4.8 and TRACWin.exe version 5.1.0 (Leblanc, 2008). The 13 HPs simulated per virtual scene were grouped in the processing software to produce one clumping factor for each retrieval method per zenith ring per scene. Here, angular clumping retrieval over a range of narrow zenith angles was a key component of the study.

Overall, angular clumping values for 24 scenes were produced for each clumping retrieval method. LX, CC, CCW and CLX were calculated for the zenith angle range 7–75°. This avoided segments less than 10 times the mean foliage element width at low zenith angles (close to nadir), and also avoided edge effects of the simulated scenes at zenith angles close to the horizon.

The LX and CLX methods were also parameterised with azimuthal segment sizes of k = 15°, 45°, and 90° applicable to HP images. Optimal segment size is an area of ongoing research and thus a range of k values were chosen in this study to be consistent with segment sizes explored in previous studies (Leblanc and Fournier, 2014; Pisek et al., 2011).

3.4. Reference clumping based on 3D modeling

Canopy element clumping can be calculated as the ratio of effective PAI 'PAIe' (e.g. where Ω = 1) to total PAI. In real forested environments the total PAI is not known *a priori*. However, the total element area of both leaf and woody elements of the virtual 3D forest model are known precisely. Therefore, the ratio of PAIe to PAI can be estimated in the virtual forest environment using the known virtual forest parameters and simulated HPs used to estimate *Pgap*. The PAIe/PAI ratio can therefore be treated as the 'reference' clumping factor, $\Omega_{ref}(\theta)$, (Leblanc and Fournier, 2014). Ω_{ref} can be used to benchmark and directly assess the accuracy of the clumping retrieval methods tested in the same virtual scenes using the same *Pgap* estimates, following Leblanc and Fournier (2014):

$$\Omega_{ref}(\theta) = -\ln[\overline{Pgap(\theta)}].\cos(\theta)/[PAI.\ G_T(\theta)] = PAIe/PAI \quad (4)$$

In order to calculate the angular reference clumping value, Ω_{ref}, the parameters of mean *Pgap* '$\overline{Pgap(\theta)}\langle errorimage\rangle$' derived from simulated scene measurements and the projection coefficient of all canopy elements '$G_T(\theta)$' must first be derived (Ross, 1981; Woodgate et al., 2015a). Here, using '$G_T(\theta)$' instead of the leaf-only projection coefficient '$G_L(\theta)$' avoids errors associated with the incorrect $G(\theta)$ application due to the presence of woody elements, see Fig. 3; (Woodgate et al., 2015a). When $Pgap(\theta)$ is retrieved over a narrow view angle, Ω_{ref} is also view angle specific. All clumping retrieval methods, including Ω_{ref}, do not distinguish between foliage and woody components, thus the derived clumping metric is referred to here as total element clumping.

Calculating the scene Ω_{ref} from the same HP-derived *Pgap* data enabled a direct comparison and test of clumping retrieval methods over coincident HP image zenith angles (e.g. 7–75°). The clumping factor difference between the retrieval methods and Ω_{ref} is equivalent to the PAI error, due to the linear relationship of clumping with PAI and LAI. For example, a 0.1 clumping factor difference between a retrieval method and Ω_{ref} equates to a 10% error in PAI.

Sensitivity of the clumping retrieval methods to scene PAI and stem clumping was established through controlling for factors during significance testing. Two-way analysis of variance (ANOVA) was conducted to detect significant differences between factors such as scene PAI value and stem distribution for clumping values. If the ANOVA revealed significant differences ($p < 0.05$), Tukey's honest significance

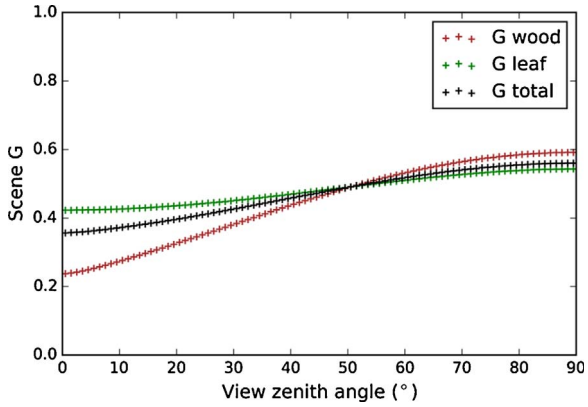

Fig. 3. Scene *G* values. Scene *G* values for leaf, wood, and combined elements. Note: for the PAI = 2.4 scenes, *G* values differed by < 0.01 across the entire view zenith angle range from the PAI = 0.6, 1.2, & 1.8 scenes, which had a slightly different tree composition. Therefore, the scene *G* values for all scenes were considered to be approximately equal.

difference (HSD) test was conducted post-hoc to determine which combination of factors had significant differences. Statistical analysis was conducted in IBM SPSS Statistics v22 (IBM Corp).

4. Results

4.1. Clumping retrieval method performance

All clumping methods from simulated HPs displayed some degree of clumping (clumping factor < 1; Fig. 4). Fig. 4 shows the total element clumping retrieval method estimates as a function of view zenith angle (for each azimuthal bin size k = 15°, 45°, 90°), compared to Ω_{ref} calculated from HPs using Eq. (4). Directly comparing the clumping retrieval methods against Ω_{ref} illustrates the magnitude of clumping factor error; proportionally equivalent to PAI error. This error is translated equivalently for LAI if a PAI to LAI conversion factor is applied. For example, a 0.1 clumping factor error equates to a 10% PAI error. Ω_{ref} for the simulated forest scenes was on average between 0.45-0.6, meaning that the assumption of a random distribution of canopy elements would lead to underestimates of PAI between 40% and 55% (Fig. 4).

Clumping factors increased with zenith angle for the LX and CLX retrieval methods (Fig. 4), with the exception of CC for PAI = 0.6 & 1.2 scenes. The CC method displayed a slight departure from linear, increasing more rapidly at larger zenith angles for scenes with PAI = 1.2, 1.8 & 2.4. LX tended to increase more rapidly for small zenith angles, before reaching an asymptote particularly in the k = 45° and 90° cases. The CLX values were more linear, with increased noise compared to the mean LX, CLX and Ω_{ref} methods. The CCW method produced simular results to the CC method. Consequently, results from the CCW method are not presented here as they did not aid in the interpretation or discussion of clumping retrieval methods tested, likely due to the fact it is an approximation of the tested CC method.

The magnitude of the error of all retrieval methods, calculated as the deviation to Ω_{ref}, typically increased with zenith angle for all k sizes (Fig. 4). The exception to this was the CC method for PAI = 0.6 scenes, where the clumping factor decreased with zenith angle. The CC and LX methods overestimated clumping values for all zenith angles and k sizes, with the exception of the LX method with k = 15° at zenith angles < 10°. At this narrow range of zenith angles, the LX method was within ± 0.02 of the mean Ω_{ref}. LX produced clumping values closer to Ω_{ref} compared with CC for all zenith angles where k = 15°, except for zenith angles > 57.5° for PAI = 0.6 scenes. This meant that the CC method removed some but not all of the large non-random gaps that were measured, thus leading to a partially clumped value that overestimated Ω_{ref}; also previously observed in comparison studies (Leblanc and Fournier, 2014; Pisek et al., 2011).

The overall best performing clumping retrieval method was CLX, which matched closest with Ω_{ref} for most zenith angles. This finding is consistent with Leblanc and Fournier (2014), who also found CLX to be the best performing clumping retrieval method in their virtual forest environments. The exception was at low zenith angles (≈7°) for scenes with PAI = 1.2, 1.8, & 2.4, with the LX (k = 15°) method performing slightly better (Fig. 4). The segment size for the LX and CLX methods which produced the closest matching clumping estimates with Ω_{ref} was k = 15°. The CC method was mainly insensitive to the k value, because k is not a parameter in the computation of the clumping factor (Eq. (3)). Increasing k led to an increased clumping factor estimated for the LX and CLX methods, consistent with findings from Leblanc and Fournier (2014) and Chianucci et al. (2014). Therefore, the increased clumping factors displayed using larger k sizes typically meant an increased difference in magnitude to Ω_{ref} and subsequent increased PAI error (Fig. 4).

The clumping factor calculated for a typical implementation of the LAI-2000/2200 instrument utilising a single measurement for each location was on average 0.98 at the 57.5° zenith angle (± 0.01 SD; Fig. 5). This clumping factor is equivalent to the LX clumping factor with k = 360°. This value overestimated Ω_{ref} by 0.5-0.6, equivalent to a 50–60% PAI underestimation.

4.2. Effect of stem distribution and PAI on clumping factors

Further investigation was undertaken to determine if the CC, LX and CLX methods could detect structural differences between the six simulated stem distributions comprising varying degrees of stem clumping. This was explored for clumping factors calculated from both the scene canopy element cover maps (θ = 0°) and simulated HPs (θ = 7–75°).

4.2.1. Scene canopy element cover maps Ω_{ref}

The canopy element cover maps (Fig. 1) show a birds-eye view of the stem distributions and different scene PAI values. As stem clumping increases (higher *v:m* values), the proportion of large gaps also visibly increases, with the largest differences observed between the Regular (*v:m* = 0.4) and Neyman (*v:m* = 5) stem distributions; the least and most clumped distributions, respectively.

Clumping factors calculated from the scene canopy element cover maps' *Pgap* data and known virtual scene parameters can be treated as reference, Ω_{ref}, at nadir. Additionally, scene cover map *Pgap* and Ω_{ref} values can be used to benchmark HP estimates, as the scene cover maps are a complete sample of the scenes whereas the HPs are only a subsample. Therefore, clumping factor and *Pgap* differences between the cover maps and HPs can be attributed to sampling effects (i.e. sensor geometry and sample location).

In theory, for the scene clumping factor to vary at zenith, the proportion of canopy element overlap would also need to vary; corresponding to the scene *Pgap* change. However, the observed *Pgap* values across different stem clumping values of the same scene PAI value were almost equivalent, thus leading to near equivalent scene Ω_{ref} (Fig. 6). Only the Regular distribution clumping factor was significantly different to the other five stem distributions when grouping the stem distributions (p < 0.02, Tukey HSD). This was exemplified in Fig. 6, with the highest clumping factor belonging to the Regular stem distribution for each scene PAI value as expected. Although scene *Pgap* was significantly different for every PAI value (p < 0.001, Tukey HSD), the scene clumping factors were not (p > 0.28, Tukey HSD). The implication of this finding is that at the 90 m x 90 m scale, the scene clumping factor was almost insensitive to the range of stem distributions tested, which encompassed the measured range at the Rushworth study site. This demonstrated that Ω_{ref} values were predominantly driven by within-crown clumping values for the Eucalypt scenes tested,

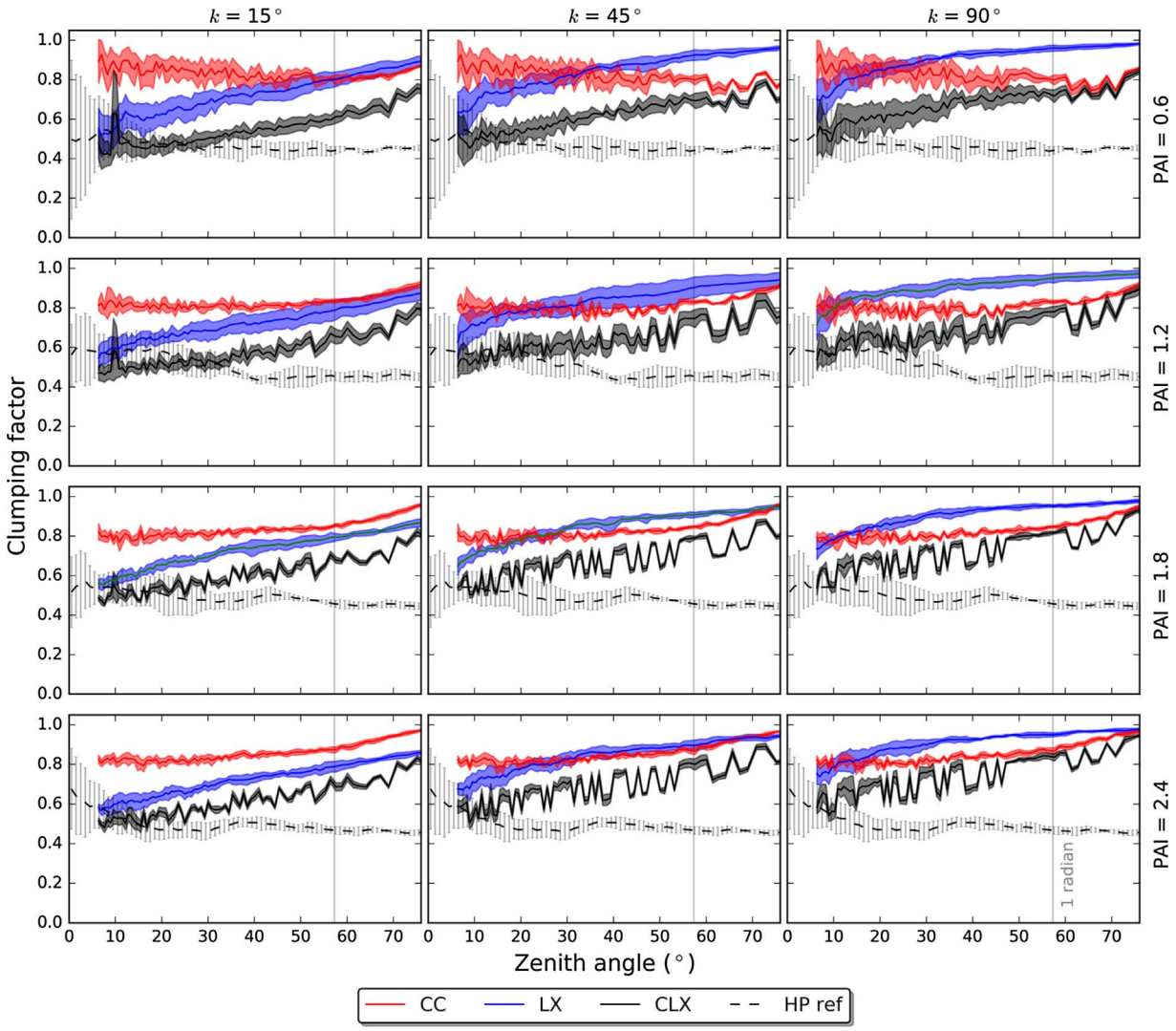

Fig. 4. Mean scene clumping estimates. Mean scene clumping estimates of the six stem distributions calculated for the clumping retrieval methods of the simulated HPs, namely; CC (red), LX (blue), and CLX (black), compared with Ω_{ref} (dashed line). Results are grouped into scene PAI value (rows: PAI = 0.6, 1.2, 1.8, 2.4) and three different segment sizes (columns: k = 15°, 45°, and 90°). Each scene comprises a specific stem distribution and PAI value, sampled from 13 HP positions. The shaded area around the CC, LX and CLX methods represents ± 1 standard deviation. Ω_{ref} was calculated as the ratio of PAIe/PAI from Eq. (4), using the known PAI, G_T, and *Pgap* from the simulated HPs calculated from the average *Pgap* of all HPs from that particular PAI scene value (n = 78). The Ω_{ref} error bars on the dashed line represent one standard deviation of Ω_{ref} calculated from the six individual stem distributions comprising the scene PAI. Accompanying mean scene *Pgap* per PAI value are presented in Fig. 3 in Woodgate et al. (2016). (For interpretation of the references to colour in this figure legend, the reader is referred to the web version of this article.)

and not by stem distribution causing minor crown overlap changes.

4.2.2. Simulated hemispherical photography

The LX and CLX clumping retrieval methods from the HPs showed slightly increased sensitivity to the six stem distributions tested in contrast to the Ω_{ref} values calculated from the cover maps (Fig. 7). For example, the most clumped stem distribution 'Neyman *v:m* 5′ typically produced the lowest clumping factor at each scene PAI value for both the LX and CLX methods, with the exception of the Random stem distribution with PAI = 1.2. Furthermore, the least clumped stem distribution, Regular *v:m* 0.5, was among the highest clumping factor for each scene PAI value, again with the exception of PAI = 1.2. Leblanc (pers. comm., 21st May, 2014) also found a small trend of increased stem clumping decreasing the clumping factor as expected for the CLX and CC retrieval methods, for the zenith angle range of 55–60° examined in Leblanc and Fournier (2014). However, in this study the CC method was insensitive to stem distribution.

4.3. Clumping bias

Departures from the expected trend of increased stem clumping leading to an increased clumping factor for the LX and CLX retrieval methods were further investigated (e.g. Fig. 7). The first anomaly explored was the Random (*v:m* 1) stem distribution scene with PAI = 1.2. This scene displayed the highest clumping factors for PAI = 1.2, even though it is theoretically the second least clumped distribution; second only to the Regular stem distribution (*v:m 0.5*). One HP sample location from the Random PAI = 1.2 stem distribution revealed about one third of the image as a tree stem (Fig. 8a). The woody-to-total plant material proportion (α) of the image was highly positively biased (α = 0.71, compared with the average of 0.37), and was one of the three outliers of the 312 simulated HPs identified in Figs. 5 and 6 from Woodgate et al. (2016). The nearby large stem led to a negatively biased *Pgap* over most zenith angles compared with the other 12 HPs from the scene (results not shown). This unrepresentative sample also biased the gap size distribution, as there were no small gaps in 1/3 of the image due to the tree stem. A consequence of the large tree in the image was the Random

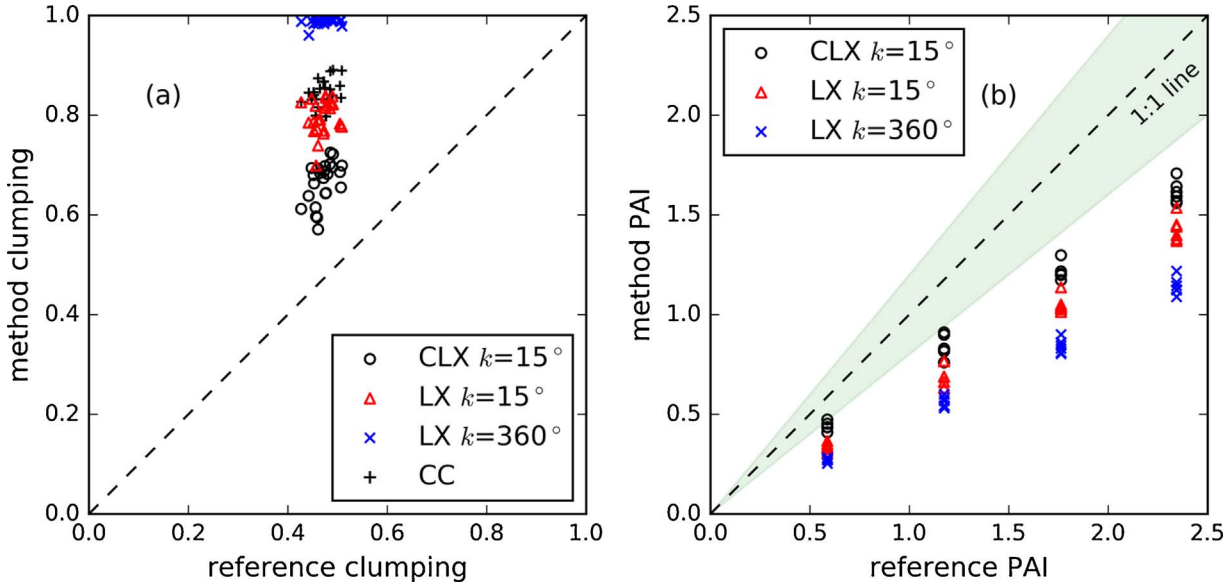

Fig. 5. Reference clumping versus method clumping factors and resulting PAI comparison. **(a)** Comparison of the CC, LX (k = 15°, 360°), and CLX (k = 15°) clumping retrieval methods with the HP Ω_{ref} at the zenith angle of 55–60°. Each individual marker represents a scene clumping factor – all 24 scenes are presented. **(b)** Corresponding PAI errors of the CLX (k = 15°) and the LX (k = 15°, 360°) clumping methods for all simulated scenes at the zenith angle of 55–60°. The shaded area represents a ± 20% error.

stem distribution scene having twice the number of null gap segments as the other stem distributions for the same scene PAI; the next closest was the Regular distribution for PAI = 1.2.

The scene clumping results were recomputed omitting the outlier image to isolate its effect. The omission of the outlier image resulted in the LX clumping factor increasing on average by between 0.05-0.15, with a slightly smaller increase of around 0.03-0.06 for CLX over all zenith angles (Fig. 8b). The recomputed clumping factors placed them in their expected position relative to the other stem distribution clumping factors from Fig. 7. This demonstrated the sensitivity of the LX and CLX clumping retrieval methods to biased gap size distributions, even though the image was only one of thirteen comprising a plot. Overall, for zenith angles less than 75°, the proportion of null gap segments was less than 1% for all k sizes (< 0.7%, < 0.2%, and < 0.02% for k = 15°, 45°, and 90°, respectively). Therefore, the potential clumping retrieval method bias caused by null gap segments was small due to the negligible fraction of null segments detected.

5. Discussion

5.1. Reference clumping angular behavior

The implication of clumping factors varying with zenith angle is that it is common to derive a single clumping factor to be representative of a plot, site or forest type (Pisek et al., 2013a). Numerous studies have demonstrated both theoretical and *in-situ* derived clumping factors to vary as a function of view zenith angle, e.g. (Piayda et al., 2015; Pisek et al., 2011; Pisek et al., 2013b; Ryu et al., 2010; Woodgate et al., 2015a). This suggests clumping factors or site-specific clumping factors should be provided with their derivation angle(s). Additionally, the clumping factor combining the correct angular values of *Pgap(θ)*, $G_T(\theta)$ and cos*(θ)* or PAIe is recommended for accurate PAI or LAI estimation. We would also expect the Ω_{ref} magnitude and trend with view zenith angle found in this study to be different for other leaf angle distributions and forest types.

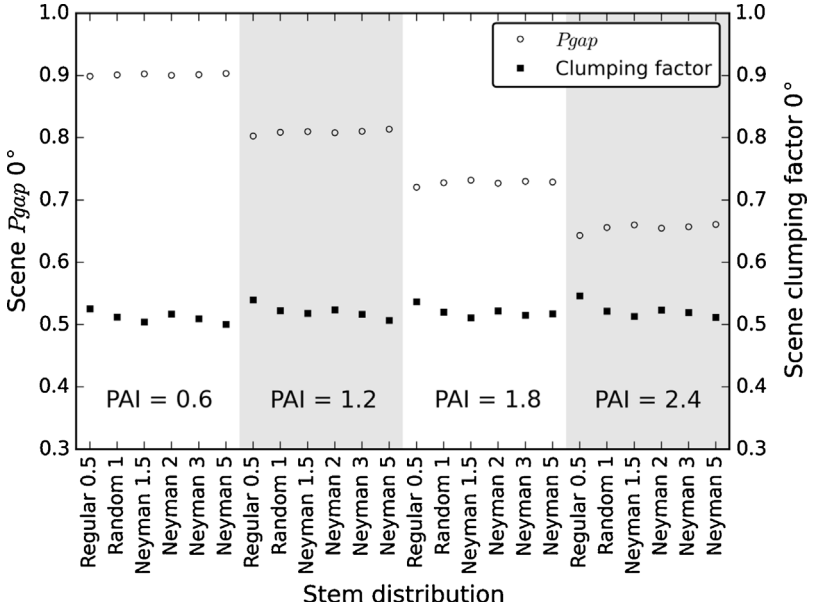

Fig. 6. Scene Pgap and reference clumping values from the canopy element cover maps. Scene *Pgap* at zenith and Ω_{ref} for each of the 24 simulated scenes, ordered by scene PAI value and *variance:mean* stem clumping ratio (lowest to highest; left to right). The open circles denote the reference *Pgap* from the canopy element cover maps Fig. 1; the black squares denote Ω_{ref} calculated from the scene reference *Pgap*, known G_T, PAI and cos(θ) Eq. (4).

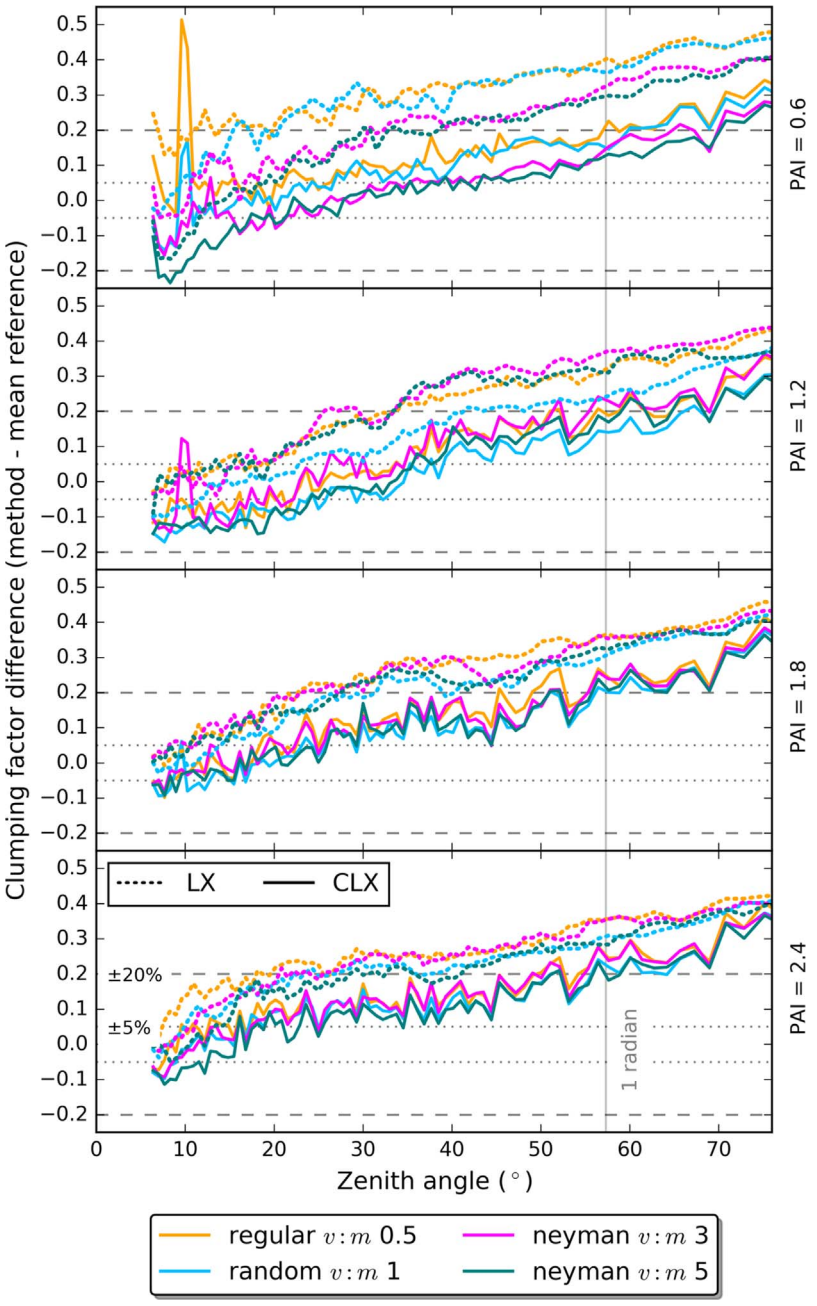

Fig. 7. Clumping retrieval method errors. Individual scene LX and CLX Ω differences from the mean HP Ω_{ref} of each scene PAI value. The mean Ω_{ref} was chosen instead of the individual scene Ω_{ref} because individual scene Ω_{ref} are highly sensitive to estimated *Pgap* and would not have revealed subtle differences in the magnitudes of the different clumping factors from the LX and CLX retrieval methods. The CLX (full colour intensity lines) and the LX (dashed lines) retrieval methods were shown for $k = 15°$; the segment size producing the most accurate results. Four stem distributions are shown, with the *variance:mean* ratio of each distribution in brackets. The neyman (*v:m* 1.5) & (*v:m* 2) stem distributions were not presented for clarity as they did not enhance results. Ω_{ref} for each scene PAI value was calculated from the average HP *Pgap* (n = 72 HPs) in addition to the known G_T and cosine of the zenith angle using Eq. (4).

The mean scene Ω_{ref} at 0° and 57.5° were within 0.05 and 0.1 of the mean within-crown clumping values for the individual tree models used (Woodgate et al., 2015a). Additionally, the average within-crown clumping values at the 0° and 57.5° viewing angles were stable, similar to the scene Ω_{ref}. Therefore, we conclude the magnitude of the scene Ω_{ref} values were mainly determined by within-crown clumping factors, not canopy element density or stem distribution. Additionally, this finding was further validated by the insensitivity of scene clumping factor to the variable stem distributions and tree densities tested (from both the cover maps and HPs). If the modelling framework was to be applied to the same canopy type with higher PAI than that tested in this study we would expect the differences between the retrieval methods and reference clumping to be even greater in accordance with the trend in Fig. 5. Additionally, in canopies with very high LAI and few intra-crown gaps (e.g. dense tropical forest), small differences in clumping will have a disproportionately large effect on retrieved LAI magnitude.

5.2. Comparison with field measured HPs

Pisek et al. (2015) published clumping values from a nearby study site (Whroo: 36° 40′S, 145° 1′E), which is part of the same patch of Box Ironbark forest on which our 3D models are based (approximately 9 km NNE of the Rushworth study site). They used the CLX ($k = 15°$) method at 57.5° to validate the performance of a global satellite-derived clumping product; described in further detail in Pisek et al. (2013a). The retrieved clumping value obtained in the field by Pisek et al. (2015) was ≈0.61 ± 0.07, which closely matched the clumping value calculated in this study (0.66 ± 0.04, Fig. 5a; calculated from the simulated HPs using the same retrieval method). Although we found the CLX method to be the most accurate method here, the clumping error was around 0.19 for the same forest patch as reported in Pisek et al. (2015). This suggests that a degree of caution must be taken when using clumping retrieval methods in forests matching (or similar to) the structural conditions of the Rushworth site, particularly at higher zenith

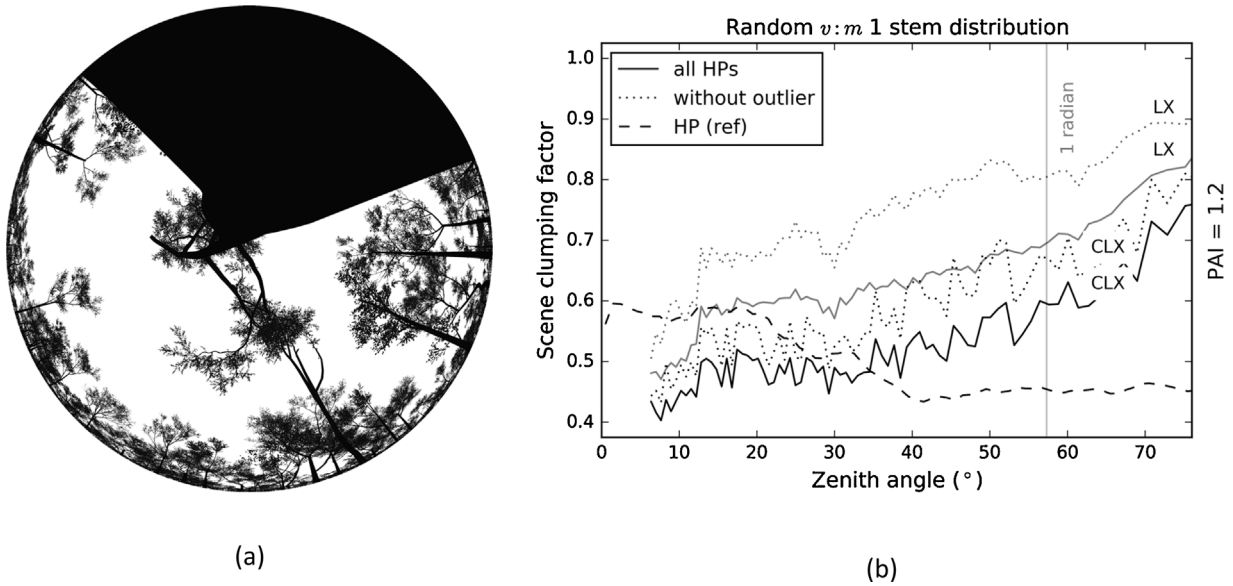

Fig. 8. Simulated HP outlier image and recalculated plot clumping retrieval methods. **(a)** Simulated HP from the PAI = 1.2 Random scene, which illustrates the large nearby stem to the image location taking up one third of the HP image (HP α = 0.71). This was the outlier image that negatively biased the scene clumping for LX and CLX for the PAI = 1.2 Random stem distribution scene. **(b)** Displays the Random stem distribution (*v*:*m* = 1) scene clumping factors for the LX (grey) and CLX (black) retrieval methods (k = 15°) from including all images (solid lines) and with the outlier image excluded from analysis (dotted lines). The scene Ω_{ref} is shown overlayed (dashed line).

angles (> 30°) where clumping from the evaluated methods is subject to larger errors (this study; Leblanc and Fournier, 2014). Other factors affecting the comparison between clumping factors include: generic 3D modelling assumptions (leaf size, leaf angle distribution etc.), image resolution, field-measured HP image classification accuracy, and sampling design to name a few.

5.3. Applications and limitations of the 3D simulation and modelling framework

The relative insensitivity of retrieved clumping factors from the CLX (k = 15°) method to a range of stem distributions and scene PAI values suggests the potential for clumping factor calibration of both ground-retrieval methods and satellite retrieval algorithms using 3D modelling. However, it is expected that the performance of these methods will vary depending on forest type, based on the architecture of the trees and relative positioning of crowns. We are unaware of other studies which benchmark retrieval methods in the same kind of simulation modelling framework we use here which utilise highly-detailed 3D reconstructed trees representative of a specific canopy or forest type. However, the complexity, resources, time, and high degree of skill required to create a representative virtual forest environment are considerable. Accurate 3D reconstructions of real-world forest environments to the required level-of-detail are expected to become more commonplace due to technology and algorithm developments (Newnham et al., 2015).

5.4. What was the cause of the clumping retrieval method angular dependence?

As LAI and clumping can be retrieved indirectly on the ground over a narrow view zenith angle range centred on different zenith angles, the retrieved clumping factors increasing as a function of zenith angle seen in this study is of significance. The significance is amplified by the different behaviour of the reference clumping, which remained stable on average across all zenith angles > 15° (Fig. 4).

Angular dependence of clumping retrieval methods applied to HP images where the clumping factor increased with zenith angle have been reported for the CC, LX and CLX algorithms from photography and TRAC instruments for a range of needle leaf and broadleaf canopies (Chen, 1996; Kucharik et al., 1999; Leblanc et al., 2005; Piayda et al., 2015; Pisek et al., 2011). Interestingly, Ryu et al. (2010) found decreasing clumping factors with increasing zenith angle from a range of methods including the CC and CLX algorithms from the TRAC instrument in a savanna, which more closely reflect the slightly decreasing reference clumping behaviour shown here (Fig. 4). However, as far as we are aware, no other studies have explored the performance of different clumping retrieval methods applied to HP images by comparing retrieved values against a known reference or 'truth', or at least not to the accuracy tested in this study using a 3D modelling framework, which included a wide range of zenith angles. Leblanc and Fournier (2014) limited their analysis to the narrow 55 − 60° zenith angle range, and with a model of much lower structural fidelity (see Appendix A). The only uncertainty source this framework contends with is that of measurement sampling (i.e. number and location of samples to representatively measure the scene domain), as all inputs of the reference clumping formula (Eq. (4)) are precisely determined or known.

Here, angular dependence of clumping factors or error linked to increasing canopy element density was considered a minor or non-issue due to the relative insensitivity of the clumping retrieval methods and Ω_{ref} to scene PAI. Therefore, an insight into why the clumping factors from the retrieval methods typically increased with zenith angle may lie in the combination of: (i) an intrinsic characteristic of HP images affecting the gap/no-gap transect length to which the clumping retrieval algorithm is applied i.e. 'segment length', and (ii) the clumping retrieval algorithm assumptions. Both explanations are further elaborated below.

For HP images, the segment length (in pixels) of the LX and CLX methods is a function of both zenith angle and azimuthal segment width 'k'. For example, k = 360° relates to the full azimuth range or entire zenith ring being incorporated as a single gap/no-gap transect (segment), which will increase in pixel length with increasing zenith angle. The LX method assumes a random spatial distribution of plant material within a segment. This assumption typically becomes less valid for increasing segment sizes in heterogeneous canopies such as forests, due to clumping occurring at all scales from the leaf or shoot right up to the stand (Chen and Cihlar, 1995a; Fournier et al., 1997). Therefore, the LX method is more applicable for clumping estimation at a scale larger than the segment size (Chianucci et al., 2014; Lang and Xiang, 1986).

Smaller k values and zenith angles close to nadir lead to a smaller

gap/no-gap sample in terms of the sampled 3D volume or 2D projected area of a scene or plot. The smaller both the k value and the zenith angle for HP images, the higher the frequency of occurrence of both low and high gap probability segments. This is caused by a smaller degree of spatial averaging of canopy elements from shorter pixel transects, which increases the variance of gap probability. This in turn leads to lower LX and CLX clumping factors (a more clumped canopy) due to the convexity of the logarithm approach to clumping estimation.

The CC method attempts to correct for the non-random gap/no-gap distribution whilst operating at the segment scale in the CLX method. This may in part explain why CLX typically performed better than LX, correcting the potential violation of an assumption of randomly distributed canopy elements within a segment of the highly clumped simulated Rushworth forest environment examined here. This also may explain the smaller observed sensitivity of CLX to k compared to LX, which was also found in Leblanc and Fournier (2014). Although the CC method does not have k as a parameter, it is instead resolved over the entire segment or length of extracted pixels from an HP image at a given zenith angle. As explained previously the number of pixels for any given k increases with zenith angle. Therefore, the longer the transect length in pixels, the more difficulty the CC method may encounter in removing non-random canopy gaps as seen for scenes with PAI = 1.2, 1.8 and 2.4 (Fig. 4). The practical considerations for choosing an optimal segment size are further discussed in Appendix B.

5.5. Practical implications for field-measured HPs

The higher clumping retrieval method errors at the approximate 57.3° viewing angle found in this study compared with accurate near-zenith estimates for LX and CLX retrieval methods presents a potential trade-off with ease of implementation in the field. At the narrow $55-60^{\circ}$ view zenith angle, both G of woody components and leaf components are expected to converge to a value of 0.5 in many forest types due to the nature of the G formulation (Nilson, 1971; Wilson, 1963; Woodgate et al., 2015a), as demonstrated in Fig. 3. However, G typically requires empirical measurements to be determined at viewing angles other than the 57.3° (Pisek et al., 2013b; Woodgate et al., 2015a). Estimating G of leaf and wood at these angles in the field is time consuming and prone to sampling errors (de Wit, 1965; Monteith, 1965; Pisek et al., 2013b; Ryu et al., 2010). Conversely, *Pgap* estimates at this larger zenith angle were more stable than view angles closer to zenith, due to increased projected HP image sample radius at larger zenith angles. Therefore, fewer measurements are required to estimate a robust *Pgap* estimate. The effects of sampling and scale are further discussed in Appendix C.

A practical implication of sampling in woody ecosystems is the presence of stems in HP images. Disproportionately large stems close to (< 1 m) the HP image location bias the gap size distribution as previously discussed. Fig. 7 exemplifies a negatively biased clumping index retrieval from LX and to a lesser extent CLX due to the presence of a large stem close to the HP image location. At the stand or plot scale, bias is likely to be higher with increasing zenith angle for the simulated forest used here due to the visible α proportion increasing with zenith angle. Unrepresentative HP sampling too close to large stem locations, typically < 1 m, resulted in both positive α and clumping factor biases in this study. Therefore, a combination of careful HP image sampling away from large tree stems, and a small segment size for which there are few or no non-gap segments is recommended.

6. Conclusions

This manuscript presents an evaluation of the indirect CC, LX, and CLX clumping retrieval methods used for LAI estimation. The method performance was assessed in a virtual forest canopy with a high degree of architectural realism, representative of a Box Ironbark Eucalypt forest in Eastern Australia. We showed that caution must be taken when benchmarking the performance of clumping methods, and subsequently LAI retrieval methods implementing these clumping methods, against other indirect methods whose performance in specific study areas or structural types remain largely untested. Special attention needs to be given to differences between the true angular clumping behaviour of a canopy and that of the clumping retrieval algorithms which return effective values, rather than true values.

The CLX clumping retrieval method with $k = 15^{\circ}$ performed best, matching the reference clumping values to within 0.1 close to nadir. Error in retrieved clumping factors increased in a near linear way with zenith angle to > 30% PAI at 75°, for all structural configurations. The performance of all clumping retrieval methods was poorer at larger zenith angles, with PAI underestimates around 25–30% on average when derived from the 55–60° zenith angle. The LX and CC methods showed even greater underestimation of PAI. Therefore, in practice, careful consideration of zenith angle range utilised from HP is recommended. In addition, we would suggest that whenever site-scale clumping factors are estimated, the zenith angle used to derive them from gap size and gap size distribution methods are also quoted.

The majority of clumping occurred at the within-crown scale in the structural configurations tested for the Eucalypt canopies investigated, which is often overlooked in studies. Ignoring the impact of canopy element clumping for the forest type studied here would lead to LAI estimation errors around 50%. This issue has strong implications for *in situ* estimation of LAI/PAI based on commonplace indirect methods tested in this study. The findings of this study impact upon indirect LAI retrieval using *Pgap* model inversion methods, operating in environments requiring correction for non-randomly distributed canopy elements.

The ability to indirectly derive clumping from indirect *in situ* methods is affected by the retrieval algorithm performance in combination with the particular instrument's ability to estimate the 'true' gap fraction and size distribution. These are a function of instrument resolution, canopy density, gap size distribution, and representativeness of sampling location(s). Therefore, we suggest more work should be done in separating the impact of sensor and sampling effects from the canopy structural effects. This is essential to ensure ground-based retrieval methods continue to improve to meet Earth Observation accuracy requirements. Specifically, suggested future work includes applying the 3D methodology to different forest types before findings presented here can be generalised, e.g. tall or multi-layered forests would be of benefit, as would including species with different woody proportions, leaf angle distributions, and crown characteristics. Additionally, the simulation and validation framework employed here could be extended to satellite remote sensing retrieval methods. Finally, canopy element clumping has been described as a complex 3D problem, which is typically approached in a 2D manner (Gonsamo et al., 2011). Therefore, the added ranging information from LiDAR sensors warrants continued investigation for clumping studies.

Acknowledgments

The authors would like to acknowledge and thank various sources that provided support for this study. The funding that supported this study came from the Australian Postgraduate Award and the Cooperative Research Centre for Spatial Information (CRC-SI). The CRC-SI's activities are funded in part by the Australian Commonwealth's Cooperative Research Centres Programme. Thanks to Craig Macfarlane for supplying the HP classification software, and to Sylvain Leblanc for supplying the clumping software and advice. M. Disney acknowledges the support of the NERC National Centre for Earth Observation (NCEO).

Appendix A

Leblanc and Fournier (2014) and this study exhibit distinct

differences in the 3D tree models structural complexity. Tree models used in this study were reconstructed to include complex internal crown architecture, which were highly clumped (Woodgate et al., 2015a). This is in contrast to Leblanc and Fournier (2014), who implemented crown envelopes as simple geometric volumes (e.g. cones, cylinders and spheroids) filled with randomly positioned foliage elements without internal branching; tapered cylinders were used as trunks. In other words, there was no intra-crown clumping ($\Omega = 1$), which has been shown to be on average between 0.5–0.6 for the tree models utilised in this study (Woodgate et al., 2015a). Other key differences between Leblanc and Fournier (2014) and our approach warrant further examination, such as the impact of vertical complexity of multiple canopy layers in some virtual scenes simulated by Leblanc and Fournier (2014).

Appendix B. Segment size *k*

The preceding paragraphs explained theoretical reasons for the increasing CC, LX and CLX clumping factors with increasing zenith angle in woody ecosystems where the reference clumping remained stable; but what is the optimal segment (k) size? Previous authors have stated the inability thus far to objectively determine an optimal k value (Gonsamo et al., 2010; Leblanc and Fournier, 2014; Pisek et al., 2011). In the absence of quantitatively recommending a universal segment size, here we describe the main practical considerations.

To satisfy the LX assumption of a random spatial distribution of foliage within a segment (k), separate treatment of within-crown and between-crown gaps would first be required in applicable canopies, as these two categories have distinct spatial distributions. In other words, segments which average large areas of both crown and between-crown area would likely invalidate the main LX assumption. Segment sizes proportionately small to the size of crowns would minimise spatial averaging occurring around the border of tree crowns. Macfarlane et al. (2007) separately treated within-crown and between-crown gaps, following the principle of large-non-random gap removal of the CC method (Leblanc, 2002). However, to account for the non-random spatial distribution of canopy elements within crowns, a segment size which divides individual tree crowns into sectors of randomly distributed canopy elements is required.

The disadvantage of small segment sizes is that the probability of null gap segments increases, where the solution to the natural logarithm of zero is undefined. The presence of tree stems and extremely dense crowns further increases the likelihood of null-gap segments. A sensible *Pgap* threshold is required for both null gap segments and very low *Pgap* segments to prevent a bias of low clumping factors than would otherwise be expected. The threshold criteria should follow that the logarithm of a *Pgap* segment shall not exceed the maximum expected PAI for a given segment size (i.e. the denominator in Eq. (1)).

To counter null gap segments, Gonsamo et al. (2010) proposed utilising the minimum segment size for which no null-gap segments occur. However, a single segment size for which all canopy element spatial distributions are random within each segment is unlikely to occur for most trees conforming to typical structural characteristics (as described in Fournier et al. (1997) for boreal species; and Jacobs (1955) for Eucalypt species). Furthermore, the presence of a single large stem prominent in an HP image (Fig. 7) or dense clump of foliage without gaps may positively bias a minimum threshold of k. In the absence of a known optimal segment size for the LX method, advocacy of the CLX method was made by Ryu et al. (2010), whereby the CC method attempts to further remove non-random gaps from the segments utilised in the LX method. The results of this study further support Ryu et al. (2010).

Appendix C. Sampling and scale

In this study, only uncertainty from sampling design (i.e. number and location of measurements) was a factor for HP *Pgap* uncertainty; here 'reference' *Pgap* was derived from ray intersection queries of an infinitely small beam per pixel in the ray-tracing model, thus avoiding classification errors. Several authors have commented that sampling design needs careful consideration, based on factors such as: canopy structure complexity, site homogeneity, horizontal plot extent, desired plot size, view zenith angle, and number of measurements (Morisette et al., 2006; Weiss et al., 2004; Woodgate et al., 2012).

HP *Pgap* at larger zenith angles for all simulated scenes was more stable due to sampling proportionately larger areas, thus providing a more robust and potentially more accurate approximation of the entire scene or plot *Pgap*. In addition, the increased spatial averaging that occurs with increased zenith angles may reflect the decreased variance in clumping values in both Ω_{ref} and the retrieval methods (Figs. 4 and 7). Further work investigating the impact of sampling design on accurate estimates of HP *Pgap* is suggested.

Scale is an important consideration when quantifying clumping. The Ω_{ref} range of the virtual scenes at nadir (0.49–0.55; Fig. 6) was much smaller than the within-crown Ω_{ref} range at nadir (0.46–0.72; (Woodgate et al., 2015a)). This was due to averaging effects when aggregating to the scene scale, also reflected by the small scene-scale *Pgap* range estimated from empirical data (Woodgate et al., 2016). It would be expected that more extreme stem clumping (v:m) values than those investigated in this study would have a stronger impact on the proportion of overlapping canopy elements; such as the extreme unrealistic case of all trees placed on top of one another. However, the range of stem clumping investigated was already more extreme than that which was measured from the stem plots at Rushworth (Woodgate et al., 2016). We conclude that the Rushworth site scene-scale Ω_{ref} factors are primarily driven by within-crown clumping and are relatively insensitive to stem distribution.

References

Armston, J.D., Denham, R.J., Danaher, T.J., Scarth, P.F., Moffiet, T.N., 2009. Prediction and validation of foliage projective cover from Landsat-5 TM and Landsat-7 ETM+ imagery. J. Appl. Remote Sens. 3.

Armston, J., 2013. Assessment of Airborne Lidar for Measuring the Structure of Forests and Woodlands in Queensland, Australia (PhD Thesis). The University of Queensland.

Bréda, N.J.J., 2003. Ground-based measurements of leaf area index: a review of methods, instruments and current controversies. J. Exp. Bot. 54 (392), 2403–2417. http://dx.doi.org/10.1093/jxb/erg263.

Chen, J.M., Black, T.A., 1991. Measuring leaf area index of plant canopies with branch architecture. Agric. For. Meteorol. 57 (1–3), 1–12.

Chen, J.M., Black, T.A., 1992. Foliage area and architecture of plant canopies from sunfleck size distributions. Agric. For. Meteorol. 60 (3–4), 249–266. http://dx.doi.org/10.1016/0168-1923(92)90040-B.

Chen, J.M., Cihlar, J., 1995a. Plant canopy gap-size analysis theory for improving optical measurements of leaf-area index. Appl. Opt. 34 (27), 6211–6222.

Chen, J.M., Cihlar, J., 1995b. Quantifying the effect of canopy architecture on optical measurements of leaf area index using two gap size analysis methods. IEEE Trans. Geosci. Remote Sens. 33 (3), 777–787.

Chen, J.M., Rich, P.M., Gower, S.T., Norman, J.M., Plummer, S., 1997. Leaf area index of boreal forests: theory, techniques, and measurements. J. Geophys. Res. 102 (D24), 29429–29443. http://dx.doi.org/10.1029/97jd01107.

Chen, J.M., Menges, C.H., Leblanc, S.G., 2005. Global mapping of foliage clumping index using multi-angular satellite data. Remote Sens. Environ. 97 (4), 447–457. http://dx.doi.org/10.1016/j.rse.2005.05.003.

Chen, J.M., 1996. Optically-based methods for measuring seasonal variation of leaf area index in boreal conifer stands. Agric. For. Meteorol. 80 (2–4), 135–163. http://dx.doi.org/10.1016/0168-1923(95)02291-0.

Chianucci, F., Macfarlane, C., Pisek, J., Cutini, A., Casa, R., 2014. Estimation of foliage clumping from the LAI-2000 plant canopy analyzer: effect of view caps. Trees 1–12.

de Wit, C.T., 1965. Photosynthesis of Leaf Canopies. Centre for Agricultural Publications and Documentation.

Disney, M.I., Lewis, P., Gomez-Dans, J., Roy, D., Wooster, M.J., Lajas, D., 2011. 3D radiative transfer modelling of fire impacts on a two-layer savanna system. Remote Sens. Environ. 115 (8), 1866–1881. http://dx.doi.org/10.1016/j.rse.2011.03.010.

Fernandes, R., Plummer, S., Nightingale, J., Baret, F., Camacho, F., Fang, H., Garrigues, S., Gobron, N., Lang, M., Lacaze, R., LeBlanc, S., Meroni, M., Martinez, B., Nilson, T., Pinty, B., Pisek, J., Sonnentag, O., Verger, A., Welles, J., Weiss, M., Widlowski, J.L., 2014. In: Schaepman-Strub, G., Román, M., Nickeson, J. (Eds.), Global Leaf Area Index Product Validation Good Practices. Version 2.0. Land Product Validation Subgroup (WGCV/CEOS).

Fournier, R.A., Rich, P.M., Landry, R., 1997. Hierarchical characterization of canopy architecture for boreal forest. J. Geophys. Res. Atmos. 102 (D24), 29445–29454.

http://dx.doi.org/10.1029/96JD03879.
Franklin, J., Michaelsen, J., Strahler, A.H., 1985. Spatial analysis of density dependent pattern in coniferous forest stands. Vegetation 64 (1), 29–36.
Frazer, G.W., Wulder, M.A., Niemann, K.O., 2005. Simulation and quantification of the fine-scale spatial pattern and heterogeneity of forest canopy structure: a lacunarity-based method designed for analysis of continuous canopy heights. For. Ecol. Manage. 214 (1–3), 65–90. http://dx.doi.org/10.1016/j.foreco.2005.03.056.
GCOS, 2011. In: In: W. M. Organization (Ed.), Systematic Observation Requirements for Satellite-based Data Products for Climate Vol. 15 GCOS, Switzerland.
Gonsamo, A., Pellikka, P., 2009. The computation of foliage clumping index using hemispherical photography. Agric. For. Meteorol. 149 (10), 1781–1787. http://dx.doi.org/10.1016/j.agrformet.2009.06.001.
Gonsamo, A., Walter, J.M.N., Pellikka, P., 2010. Sampling gap fraction and size for estimating leaf area and clumping indices from hemispherical photographs. Can. J. For. Res. 40 (8), 1588–1603.
Gonsamo, A., Walter, J.-M.N., Pellikka, P., 2011. CIMES: a package of programs for determining canopy geometry and solar radiation regimes through hemispherical photographs. Comput. Electron. Agric. 79 (2), 207–215. http://dx.doi.org/10.1016/j.compag.2011.10.001.
Jacobs, M.R., 1955. Growth Habits of the Eucalypts. Forestry and Timber Bureau, Canberra.
Jonckheere, I., Fleck, S., Nackaerts, K., Muys, B., Coppin, P., Weiss, M., Baret, F., 2004. Review of methods for in situ leaf area index determination Part I. Theories, sensors and hemispherical photography. Agric. For. Meteorol. 121 (1–2), 19–35. http://dx.doi.org/10.1016/j.agrformet.2003.08.027.
Jonckheere, I., Nackaerts, K., Muys, B., van Aardt, J., Coppin, P., 2006. A fractal dimension-based modelling approach for studying the effect of leaf distribution on LAI retrieval in forest canopies. Ecol. Modell. 197 (1–2), 179–195. http://dx.doi.org/10.1016/j.ecolmodel.2006.02.036.
Jupp, D.L.B., Culvenor, D.S., Lovell, J.L., Newnham, G.J., Strahler, A.H., Woodcock, C.E., 2009. Estimating forest LAI profiles and structural parameters using a ground-based laser called 'Echidna®'. Tree Physiol. 29 (2), 171–181.
Kalácska, M., Calvo-Alvarado, J.C., Sánchez-Azofeifa, G.A., 2005. Calibration and assessment of seasonal changes in leaf area index of a tropical dry forest in different stages of succession. Tree Physiol. 25 (6), 733–744.
Kucharik, C.J., Norman, J.M., Gower, S.T., 1999. Characterization of radiation regimes in nonrandom forest canopies: theory, measurements, and a simplified modeling approach. Tree Physiol. 19 (11), 695–706.
LI-COR. (2011). LAI-2200 Plant Canopy Analyser Instruction Manual.
Lang, A.R.G., Xiang, Y., 1986. Estimation of leaf area index from transmission of direct sunlight in discontinuous canopies. Agric. For. Meteorol. 37 (3), 229–243. http://dx.doi.org/10.1016/0168-1923(86)90033-x.
Law, B.E., Cescatti, A., Baldocchi, D.D., 2001. Leaf area distribution and radiative transfer in open-canopy forests: implications for mass and energy exchange. Tree Physiol. 21 (12–13), 777–787. http://dx.doi.org/10.1093/treephys/21. 12-13.777.
Leblanc, S.G., Chen, J.M., 2001. A practical scheme for correcting multiple scattering effects on optical LAI measurements. Agric. For. Meteorol. 110 (2), 125–139. http://dx.doi.org/10.1016/s0168-1923(01)00284-2.
Leblanc, S.G., Fournier, R.A., 2014. Hemispherical photography simulations with an architectural model to assess retrieval of leaf area index. Agric. For. Meteorol. 194 (0), 64–76. http://dx.doi.org/10.1016/j.agrformet.2014.03.016.
Leblanc, S.G., Chen, J.M., Fernandes, R., Deering, D.W., Conley, A., 2005. Methodology comparison for canopy structure parameters extraction from digital hemispherical photography in boreal forests. Agric. For. Meteorol. 129 (3–4), 187–207. http://dx.doi.org/10.1016/j.agrformet.2004.09.006.
Leblanc, S.G., 2002. Correction to the plant canopy gap-size analysis theory used by the tracing radiation and architecture of canopies instrument. Appl. Opt. 41 (36), 7667–7670. http://dx.doi.org/10.1364/AO.41.007667.
Leblanc, S., 2008. DHP-TRACWin Manual (Vol. 1.0.3. Natural Resources Canada, Canada Centre for Remote Sensing, Centre Spatial John H. Chapman, Québec, Canada.
Lewis, P., 1999. Three-dimensional plant modelling for remote sensing simulation studies using the botanical plant modelling system. Agronomie 19 (3–4), 185–210.
Macfarlane, C., Hoffman, M., Eamus, D., Kerp, N., Higginson, S., McMurtrie, R., Adams, M., 2007. Estimation of leaf area index in eucalypt forest using digital photography. Agric. For. Meteorol. 143 (3-4), 176–188. http://dx.doi.org/10.1016/j.agrformet.2006.10.013.
Miller, E.E., Norman, J.M., 1971. A sunfleck theory for plant canopies I. Lengths of sunlit segments along a transect. Agron. J. 63 (5), 735–738. http://dx.doi.org/10.2134/agronj1971.00021962006300050024x.
Monsi, M., Saeki, T., 1965. On the factor light in plant communities and its importance for matter production. Ann. Bot. 95 (3), 549–567. http://dx.doi.org/10.1093/aob/mci052.
Monteith, J., 1965. Light distribution and photosynthesis in field crops. Ann. Bot. 29 (1), 17–37.
Morisette, J.T., Baret, F., Privette, J.L., Myneni, R.B., Nickeson, J.E., Garrigues, S., Shabanov, N.V., Weiss, M., Fernandes, R.A., Leblanc, S.G., Kalacska, M., Sánchez-Azofeifa, G.A., Chubey, M., Rivard, B., Stenberg, P., Rautiainen, M., Voipio, P., Manninen, T., Pilant, A.N., Lewis, T.E., Iiames, J.S., Colombo, R., Meroni, M., Busetto, L., Cohen, W.B., Turner, D.P., Warner, E.D., Petersen, G.W., Seufert, G., Cook, R., 2006. Validation of global moderate-resolution LAI products: a framework proposed within the CEOS land product validation subgroup. IEEE Trans. Geosci. Remote Sens. 44 (7), 1804–1814. http://dx.doi.org/10.1109/tgrs.2006.872529.
Newnham, G.J., Armston, J.D., Calders, K., Disney, M.I., Lovell, J.L., Schaaf, C.B., Strahler, A.H., Danson, F.M., 2015. Terrestrial laser scanning for plot-scale forest measurement. Curr. For. Rep. 1 (4), 239–251. http://dx.doi.org/10.1007/s40725-015-0025-5.
Neyman, J., 1939. On a new class of contagious distributions, applicable in entomology and bacteriology. Ann. Math. Stat. 10 (1), 35–57. http://dx.doi.org/10.2307/2235986.
Nilson, T., 1971. A theoretical analysis of the frequency of gaps in plant stands. Agric. Meteorol. 8 (C), 25–38.
Nilson, T., 1999. Inversion of gap frequency data in forest stands. Agric. For. Meteorol. 98–99, 437–448. http://dx.doi.org/10.1016/s0168-1923(99)00114-8.
Piayda, A., Dubbert, M., Werner, C., Vaz Correia, A., Pereira, J.S., Cuntz, M., 2015. Influence of woody tissue and leaf clumping on vertically resolved leaf area index and angular gap probability estimates. For. Ecol. Manage. 340 (0), 103–113. http://dx.doi.org/10.1016/j.foreco.2014.12.026.
Pielou, E.C., 1962. Runs of one species with respect to another in transects through plant populations. Biometrics 18 (4), 579–593. http://dx.doi.org/10.2307/2527903.
Pisek, J., Lang, M., Nilson, T., Korhonen, L., Karu, H., 2011. Comparison of methods for measuring gap size distribution and canopy nonrandomness at Järvselja RAMI (RAdiation transfer Model Intercomparison) test sites. Agric. For. Meteorol. 151 (3), 365–377. http://dx.doi.org/10.1016/j.agrformet.2010.11.009.
Pisek, J., Ryu, Y., Sprintsin, M., He, L., Oliphant, A.J., Korhonen, L., Kuusk, J., Kuusk, A., Bergstrom, R., Verrelst, J., Alikas, K., 2013a. Retrieving vegetation clumping index from multi-angle imaging spectroradiometer (MISR) data at 275 m resolution. Remote Sens. Environ. 138, 126–133. http://dx.doi.org/10.1016/j.rse.2013.07.014(/DOI.
Pisek, J., Sonnentag, O., Richardson, A.D., Mõttus, M., 2013b. Is the spherical leaf inclination angle distribution a valid assumption for temperate and boreal broadleaf tree species? Agric. For. Meteorol. 169, 186–194. http://dx.doi.org/10.1016/j.agrformet.2012.10.011.
Pisek, J., Govind, A., Arndt, S.K., Hocking, D., Wardlaw, T.J., Fang, H., Matteucci, G., Longdoz, B., 2015. Intercomparison of clumping index estimates from POLDER, MODIS, and MISR satellite data over reference sites. ISPRS J. Photogramm. Remote Sens. 101 (0), 47–56. http://dx.doi.org/10.1016/j.isprsjprs.2014.11.004.
Ross, J., 1981. The Radiation Regime and Architecture of Plant Stands. Junk, London.
Ryu, Y., Sonnentag, O., Nilson, T., Vargas, R., Kobayashi, H., Wenk, R., Baldocchi, D.D., 2010. How to quantify tree leaf area index in an open savanna ecosystem: a multi-instrument and multi-model approach. Agric. For. Meteorol. 150 (1), 63–76. http://dx.doi.org/10.1016/j.agrformet.2009.08.007.
Schaefer, M.T., Farmer, E., Soto-Berelov, M., Woodgate, W., Jones, S., 2015. Overview of ground based techniques for estimating LAI. In: Soto-Berelov, M., Held, A., Phinn, S., Jones, S. (Eds.), AusCover Good Practice Guidelines: A Technical Handbook Supporting Calibration and Validation Activities of Remotely Sensed Data Products. TERN AusCover, pp. 88–118. http://data.auscover.org.au/xwiki/bin/view/Good+Practice+Handbook/WebHome.
Spanner, M.A., Pierce, L.L., Peterson, D.L., Running, S.W., 1990. Remote sensing of temperate coniferous forest leaf area index. The influence of canopy closure, understory vegetation and background reflectance. Int. J. Remote Sens. 11 (1), 95–111.
Walter, J.M.N., Fournier, R.A., Soudani, K., Meyer, E., 2003. Integrating clumping effects in forest canopy structure: an assessment through hemispherical photographs. Can. J. Remote Sens. 29 (3), 388–410.
Weiss, M., Baret, F., Smith, G.J., Jonckheere, I., Coppin, P., 2004. Review of methods for in situ leaf area index (LAI) determination: part II. Estimation of LAI, errors and sampling. Agric. For. Meteorol. 121 (1–2), 37–53. http://dx.doi.org/10.1016/j.agrformet.2003.08.001.
Widlowski, J.-L., Mio, C., Disney, M., Adams, J., Andredakis, I., Atzberger, C., Brennan, J., Busetto, L., Chelle, M., Ceccherini, G., Colombo, R., Côté, J.-F., Eenmäe, A., Essery, R., Gastellu-Etchegorry, J.-P., Gobron, N., Grau, E., Haverd, V., Homolová, L., Huang, H., Hunt, L., Kobayashi, H., Koetz, B., Kuusk, A., Kuusk, J., Lang, M., Lewis, P.E., Lovell, J.L., Malenovský, Z., Meroni, M., Morsdorf, F., Mõttus, M., Ni-Meister, W., Pinty, B., Rautiainen, M., Schlerf, M., Somers, B., Stuckens, J., Verstraete, M.M., Yang, W., Zhao, F., Zenone, T., 2015. The fourth phase of the radiative transfer model intercomparison (RAMI) exercise: actual canopy scenarios and conformity testing. Remote Sens. Environ. 169, 418–437. http://dx.doi.org/10.1016/j.rse.2015.08.016.
Wilson, J., 1963. Estimation of foliage denseness and foliage angle by inclined point quadrats. Aust. J. Bot. 11 (1), 95–105. http://dx.doi.org/10.1071/BT9630095.
Woodgate, W., Soto-Berelov, M., Suarez, L., Jones, S., Hill, M.J., Wilkes, P., Axelsson, C., Haywood, A., Mellor, A., 2012. Searching for an optimal sampling design for measuring LAI in an upland rainforest. In: Paper Presented at the Geospatial Science Research Symposium GSR2. Melbourne.
Woodgate, W., Disney, M., Armston, J.D., Jones, S.D., Suarez, L., Hill, M.J., Wilkes, P., Soto-Berelov, M., Haywood, A., Mellor, A., 2015a. An improved theoretical model of canopy gap probability for Leaf Area Index estimation in woody ecosystems. For. Ecol. Manage. 358, 303–320. http://dx.doi.org/10.1016/j.foreco.2015.09.030.
Woodgate, W., Jones, S.D., Suarez, L., Hill, M.J., Armston, J.D., Wilkes, P., Soto-Berelov, M., Haywood, A., Mellor, A., 2015b. Understanding the variability in ground-based methods for retrieving canopy openness, gap fraction, and leaf area index in diverse forest systems. Agric. For. Meteorol. 205 (0), 83–95. http://dx.doi.org/10.1016/j.agrformet.2015.02.012.
Woodgate, W., Armston, J.D., Disney, M., Jones, S.D., Suarez, L., Hill, M.J., Wilkes, P., Soto-Berelov, M., 2016. Quantifying the impact of woody material on leaf area index estimation from hemispherical photography using 3D canopy simulations. Agric. For. Meteorol. 226–227, 1–12. http://dx.doi.org/10.1016/j.agrformet.2016.05.009.
Zhao, F., Strahler, A.H., Schaaf, C.L., Yao, T., Yang, X., Wang, Z., Schull, M.A., Román, M.O., Woodcock, C.E., Olofsson, P., Ni-Meister, W., Jupp, D.L.B., Lovell, J.L., Culvenor, D.S., Newnham, G.J., 2012. Measuring gap fraction, element clumping index and LAI in Sierra Forest stands using a full-waveform ground-based lidar. Remote Sens. Environ. 125 (0), 73–79. http://dx.doi.org/10.1016/j.rse.2012.07.007.
Zheng, G., Moskal, L.M., 2009. Retrieving leaf area index (LAI) using remote sensing: theories, methods and sensors. Sensors 9 (4), 2719–2745.